NRC Research Press

ARTICLE

Suffusion susceptibility investigation by energy-based method and statistical analysis

Van Thao Le, Didier Marot, Abdul Rochim, Fateh Bendahmane, and Hong Hai Nguyen

Abstract: Internal erosion is one of the main causes of instabilities within hydraulic earth structures. Four internal erosion processes can be distinguished, and this study deals with the process of suffusion, which corresponds to the coupled processes of detachment–transport–filtration of the soil's fine fraction between the coarse fraction. Because of the great length of earth structures and the heterogeneities of soils, it is very difficult to characterize the suffusion susceptibility of the different soils. Nevertheless, a statistical analysis can be performed to optimize the experimental campaign. By using a dedicated erodimeter, an experimental program was set up to study suffusion susceptibility of 31 specimens of nonplastic and low-plasticity soils. The suffusion susceptibility is determined by the erosion resistance index, which relates the total loss of mass with the total energy expended by the seepage flow. Fourteen physical parameters are selected, and a multi-variate statistical analysis leads to a correlation between the erosion resistance index and all these parameters. A statistical analysis is performed to identify the main parameters and to focus on those that can easily be measured on existing structures. By distinguishing gap-graded and widely graded soils, two correlations are proposed to estimate the erosion resistance index.

Key words: laboratory testing, suffusion, physical parameter, statistical analysis, energy.

Résumé : L'érosion interne est l'une des principales causes des instabilités dans les ouvrages hydrauliques en terre. Quatre processus d'érosion interne peuvent être distingués et cette étude porte sur le processus de suffusion qui correspond aux processus couplés de détachement–transport–filtration de la fraction fine du sol entre les grains de la fraction grossière. En raison du grand linéaire des ouvrages en terre et des hétérogénéités des sols, il est très difficile de caractériser la susceptibilité à la suffusion des différents sols. Néanmoins, une analyse statistique peut être effectuée afin d'optimiser la campagne expérimentale. À l'aide d'un érodimètre dédié, un programme expérimental a été réalisé pour étudier la susceptibilité à la suffusion de 31 échantillons de sols non plastiques ou de faible plasticité. La susceptibilité à la suffusion est déterminée par l'indice de résistance à l'érosion, qui relie la perte de masse totale avec l'énergie totale dissipée par l'écoulement interstitiel. Quatorze paramètres physiques sont sélectionnés et une analyse statistique multivariée abouti à une corrélation entre l'indice de résistance à l'érosion et l'ensemble de ces paramètres. Une analyse statistique est effectuée afin d'identifier les principaux paramètres tout en privilégiant les paramètres aisément mesurables sur les ouvrages existants. En distinguant les sols de distributions granulométriques discontinue et continue, deux corrélations sont proposées pour estimer l'indice de résistance à l'érosion. [Traduit par la Rédaction]

Mots-clés : essais en laboratoire, suffusion, paramètre physique, analyse statistique, énergie.

Introduction

Internal erosion is one of the main causes of instabilities within hydraulic earth structures such as dams, dikes, or levees (Foster et al. 2000). According to Fell and Fry (2013), there are four types of internal erosion: concentrated leak erosion, backward erosion, contact erosion, and suffusion. Concentrated leak erosion may occur through a crack or hydraulic fracture in cohesive soils. Backward erosion mobilizes all the grains in regressive way (i.e., from the downstream part of earth structure to the upstream part) and includes backward erosion piping and global backward erosion. Contact erosion occurs where a coarse soil is in contact with a fine soil. The phenomenon of suffusion corresponds to the process of detachment and then transport of the finest particles within the porous network of cohesionless soils. The nature of the soil in the earth structure and the boundary conditions (i.e., the presence or not of a downstream filter, of cracks or interfaces with other types of soils) determine soil vulnerability to each internal erosion process. Thus, the soil erodibility must be identified, taking into account all four internal erosion processes.

For the first three aforementioned processes of internal erosion, different classifications exist to evaluate the soil erodibility, whereas in the case of suffusion, only one susceptibility classification is available and has been recently proposed by Marot et al. (2016). The absence of several suffusion susceptibility classifications may be due to the complexity of this process, which appears

Received 8 January 2017. Accepted 1 June 2017.

V.T. Le. Institut de Recherche en Génie Civil et Mécanique, Université de Nantes, 58 rue Michel Angle, BP 420, F-44606 Saint-Nazaire cedex, France; University of Science and Technology – The University of Danang, 54 Nguyen Luong Bang Street, Lien Chieu District, Da Nang City, Vietnam.
D. Marot and F. Bendahmane. Institut de Recherche en Génie Civil et Mécanique, Université de Nantes, 58 rue Michel Angle, BP 420, F-44606 Saint-Nazaire cedex, France.
A. Rochim. Institut de Recherche en Génie Civil et Mécanique, Université de Nantes, 58 rue Michel Angle, BP 420, F-44606 Saint-Nazaire cedex, France; Civil Engineering Department, Sultan Agung Islamic University, Indonesia.
H.H. Nguyen. University of Science and Technology – The University of Danang, 54 Nguyen Luong Bang Street, Lien Chieu District, Da Nang City, Vietnam.

Corresponding author: Didier Marot (email: didier.marot@univ-nantes.fr).

as the result of the coupled processes: detachment–transport–filtration of a part of the finest fraction within the porous network. For this classification, the cumulative energy expended by the seepage flow is computed, and the induced erosion is evaluated by the cumulative loss of dry mass. Six categories of soil erodibility are proposed from very resistant to very erodible.

Soils of hydraulic earth structures and their foundations are characterized by great heterogeneities (e.g., 8000 km of dikes in France and 13 200 km of dikes in Vietnam). Owing to this spatial variability of soils, the soil erodibility characterization requires a large number of erosion tests. In consequence, a statistical analysis is conducted for assessing the relationship between suffusion susceptibility and other properties of soils. By focusing on easily measurable parameters, this study contributes to an experimental campaign optimization.

To cover a large range of soil erodibility, 18 nonplastic and low-plasticity soils are selected, and a total of 31 specimens are prepared. By using a dedicated erodimeter, the erodibility is evaluated for all specimens and test results are interpreted by the energy method. The suffusion susceptibility of all tested specimens is evaluated thanks to the erosion resistance index. Two tests are performed under identical conditions to verify the repeatability. The bibliographic study permits identification of 14 predominant physical parameters that influence the soil suffusion susceptibility and that can be measured for soils of existing earth structures. A principal component analysis is performed to determine the linear correlations between the erosion resistance index and these physical parameters. By eliminating the variables that are correlated or seem meaningless owing to their redundant information with other variables on one hand, and by focusing on easily measurable parameters on the other hand, a new multivariable analysis allows building a correlation with a reduced number of physical parameters.

Background regarding experimental studies on suffusion

Identification of predominant parameters

Garner and Fannin (2010) describe the main initiation conditions for suffusion with the aid of a diagram comprising three components: material susceptibility, critical stress condition, and critical hydraulic load. In the same manner, Fell and Fry (2013) highlight three criteria that have to be satisfied for suffusion to occur: geometric criterion, stress criterion, and hydraulic criterion. The first two criteria are associated with the fabric of granular soils, and for nonplastic or low-plasticity soils, soil fabric mainly depends on the grain-size distribution, the particle shape, and soil density. The soils that are likely to suffer from suffusion are, according to Fell and Fry (2007), "internally unstable", i.e., their grain-size distribution curve is either discontinuous or upwardly concave. Based on this information, several criteria have been proposed in literature. In 1953, the U.S. Army Corps of Engineers proposed to define the stability boundary by the uniformity coefficient C_u equal to 20. One of the most widely used criterion in literature to assess the internal stability of granular soils is the Kenney and Lau's (1985) criterion. This criterion is based on the ratio H/F, where H is the mass fraction of a grain-size distribution ranging from a diameter d to $4d$, and F is the mass fraction of particles finer than d. If the minimum value of this ratio, min(H/F), is smaller than 1.3 (revised to 1.0 by Kenney and Lau 1986), then the soil is classified as internally unstable.

For the interpretation of 20 suffusion tests, Wan and Fell (2008) used three criteria for predicting the initiation of suffusion. They concluded that these methods, based on particle-size distribution, are conservative, and they proposed a method for assessing internal instability of broadly graded silt–sand–gravel soils. This method is based on two ratios: d_{90}/d_{60} and d_{20}/d_5 (where d_{90}, d_{60}, d_{20}, and d_5 are the sieve sizes for which 90%, 60%, 20%, and 5%, respectively, of the weighed soil is finer). More recently, Chang and Zhang (2013) proposed three categories of soil erodibility from the comparison of three criteria. They distinguished widely graded and gap-graded soils. Chang and Zhang defined P as the mass fraction of particles finer than 0.063 mm, and in the case of gap-graded soil, the gap ratio as $G_r = d_{max}/d_{min}$ (d_{max} and d_{min} are maximal and minimal particle sizes characterizing the gap in the grading curve, respectively). For P less than 10%, the authors assumed that the stability is correctly assessed using the criterion $G_r < 3$. For P higher than 35%, the gap-graded soil is reputed stable, and with P in the range 10%–35%, the soil is stable if $G_r < 0.3P$. According to Chang and Zhang, their method is only applicable to low-plasticity soils. From the comparisons of criteria realized by Li and Fannin (2008), Wan and Fell (2008), and Chang and Zhang (2013), Marot et al. (2016) identified the less conservative criteria for potential susceptibility to suffusion for cohesionless soils and clayey sands.

However, for the same granular distribution, suffusion tests performed on different mixtures of low percentages of kaolin with aggregates showed that angularity of coarse fraction grains contributes to increase of suffusion resistance (Marot et al. 2012). Thus, the shape of grains also plays an important role on suffusion susceptibility. Marot et al. (2012) used three methods for characterizing grain shape: digital picture analyses, direct shear tests, and by gravitating flows with a sand angulometer. Whatever indicator was considered for grain-shape characterizing, the same relative classification of the tested aggregates was obtained. However, the measurement of internal friction angle under the same density index I_d ($I_d = (e_{max} - e)/(e_{max} - e_{min})$, where e_{max}, e_{min} are the maximum and minimum values, respectively, of the void ratio e) appears to be more appropriate to characterize the influence of the grain shape on the process of suffusion.

In addition to material susceptibility, the stress condition also can influence the suffusion susceptibility. Several tests performed in oedometric conditions on unstable soils showed that a rise in the effective stress causes an increase of the soils' resistance to suffusion (Moffat and Fannin 2006). In the same manner, when tests were carried out under isotropic confinement (Bendahmane et al. 2008), the increase in the confinement pressure and the subsequence local increase of soil density (i.e., smaller size of constrictions between coarse grains) allowed a decrease in the suffusion rate.

The third condition for suffusion initiation is related to the hydraulic loading on the grains, which is often described by three distinct parameters: the hydraulic gradient, the hydraulic shear stress, and the pore velocity. The critical values of these three quantities can then be used to characterize the suffusion initiation (Skempton and Brogan 1994; Moffat and Fannin 2006; Perzlmaier 2007 among others). However, a fraction of the detached particles can re-settle or be filtered at the bulk of the porous network (Reddi et al. 2000; Bendahmane et al. 2008; Marot et al. 2009, 2011*a*; Nguyen et al. 2012; Luo et al. 2013). The processes of detachment, transport, and filtration of fine particles are thus inseparable. These processes can eventually induce local clogging, accompanied by variations of fluid velocity and interstitial pressure. Therefore, variations of both seepage flow and pressure gradient have to be taken into account to evaluate the hydraulic loading during suffusion development.

Suffusion susceptibility classification

Further to results of concentrated leak erosion tests, Marot et al. (2011*b*) proposed a new analysis based on the energy expended by the seepage flow, which is a function of both the flow rate and the pressure gradient. Three assumptions were used: the fluid temperature is assumed constant, the system is considered as adiabatic, and only a steady state is considered. The energy conservation equation permits expression of the total flow power as the summation of the power transferred from the fluid to the

Fig. 1. Schematic diagram of dedicated erodimeter. Specimen dimensions: 50 mm in diameter; 50–100 mm in height.

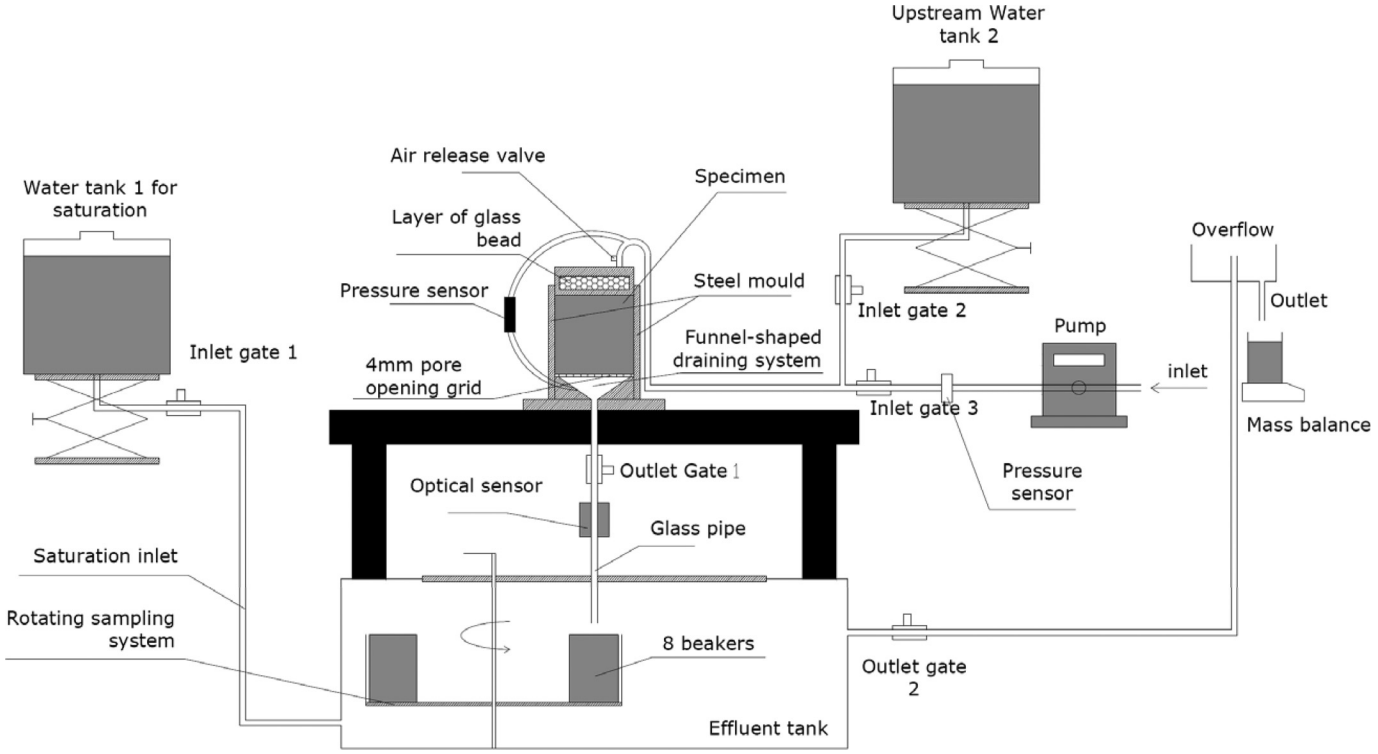

solid particles and the power dissipated by viscous stresses in the bulk. As the transfer appears negligible in the case of suffusion (Sibille et al. 2015), the authors suggest characterizing the fluid loading from the total flow power, P_{flow} (W), which is expressed by

$$(1) \qquad P_{flow} = (\gamma_w \Delta z + \Delta P)Q$$

where γ_w (N/m^3) is the specific weight of water; $\Delta z = z_A - z_B$ (m), where z_A and z_B are the vertical coordinates of the upstream section A and the downstream section B of the soil volume, respectively; $\Delta P = P_A - P_B$ (N/m^2) is the pressure drop between the sections A and B, respectively; and Q (m^3/s) is the volumetric water flow rate.

$\Delta z > 0$ if the flow is in a downward direction, $\Delta z < 0$ if the flow is upward, and the erosion power is equal to $Q\Delta P$ if the flow is horizontal.

The expended energy E_{flow} (J) is the time integration of the instantaneous power dissipated by the water seepage for the test duration (s). For the same duration, the cumulative loss of dry mass is determined, and the erosion resistance index is expressed by

$$(2) \qquad I_\alpha = -\log\left(\frac{\text{cumulative loss of dry mass}}{E_{flow}}\right)$$

Depending on the values of I_α, Marot et al. (2016) proposed six categories of suffusion susceptibility from highly erodible to highly resistant (corresponding susceptibility categories: highly erodible for $I_\alpha < 2$; erodible for $2 \le I_\alpha < 3$; moderately erodible for $3 \le I_\alpha < 4$; moderately resistant for $4 \le I_\alpha < 5$; resistant for $5 \le I_\alpha < 6$; and highly resistant for $I_\alpha \ge 6$).

Experimental investigation

Specific device for erodibility characterization

A triaxial erodimeter was designed to apply seepage flow on intact soil samples. A detailed description of the device was reported by Bendahmane et al. (2008), and a brief summary is provided hereafter.

As shown in Fig. 1, the testing apparatus comprises a modified triaxial cell, a water supply system, a soil collection system, and a water collection system. The modified triaxial cell permits the sample to become saturated in an upward direction and the fluid to be forced through the sample in a downward direction during the erosion phase. The seepage flow is applied in a downward direction to catch the eroded particles more easily. A pressure sensor is connected between the top and bottom of the specimen to measure the pressure drop between upstream and downstream. The system to generate seepage flow under constant hydraulic gradient comprises an upstream water tank. The system to generate seepage flow in flow-rate-controlled conditions comprises a gear pump connected to a pressure sensor at its outlet. For both types of hydraulic loading, the fluid circulates into the top cap, which contains a layer of glass beads to diffuse the fluid uniformly on the specimen top surface. The sample is supported by a lower grid where different wire meshes can be placed to take into account the effect of pore opening size on internal erosion (Marot et al. 2009). For this study, the opening size of the selected mesh screen is 4 mm to allow the migration of all grains and to reproduce in situ earth structures without filter, as a dike for example. The funnel-shaped draining system is connected to the effluent tank by a glass pipe. In the case of silt or clay suffusion, a multi-channel optical sensor is placed around the glass pipe (Marot et al. 2011*a*). Thanks to a previous calibration, the optical sensor allows measuring the silt or clay concentration within the effluent, which is expressed as the ratio of the mass of fine particles to water mass within the fluid with a maximum relative error of 5% (Marot et al 2011*a*). The time integration of the fine-particle concentration gives the cumulative eroded dry mass for the corresponding duration (Bendahmane et al. 2008) with a maximum relative error of 7%. Moreover, the detection of sand grains in the effluent is assessed thanks to the comparison of the voltages of each light-emitting diode (LED) of the optical sensor (Marot et al. 2011*a*). For a high value of silt concentration within the effluent or

Fig. 2. Grain-size distribution of (*a*) soils R1, R2, 3, CH-5, CH-10, B, 6, CD, and (*b*) strongly gap-graded soils 1, DR-C, G3-11, G3-13, G3-14, C, DR-A, DR-B, 4, 5. [Colour online.]

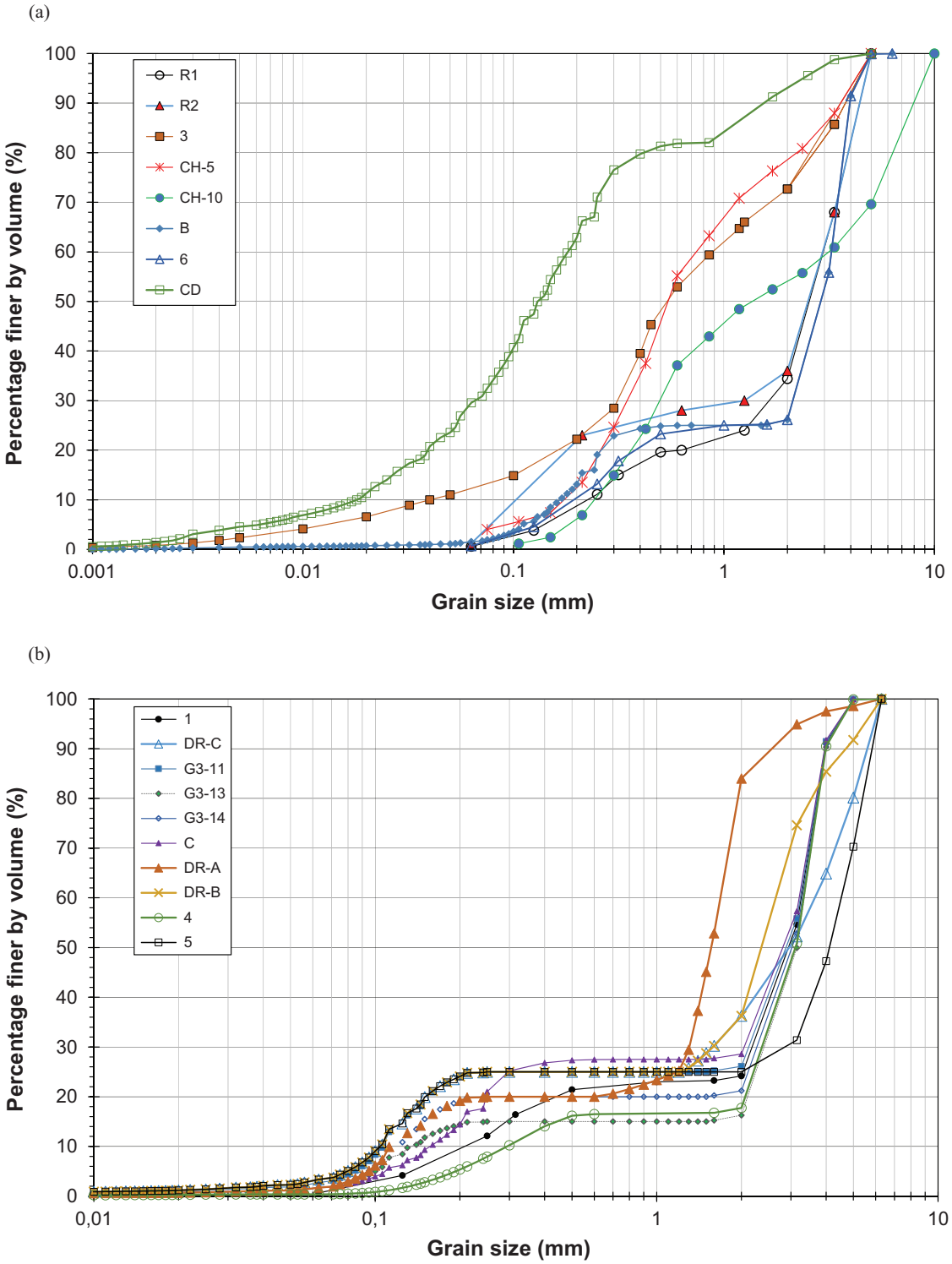

when the effluent contains sand grains, the solid mass measurement can be performed by continuous weighing, as mass accuracy of a few milligrams is sufficient. The effluent tank is equipped with an overflow outlet (to control the downstream hydraulic head) and a rotating sampling system containing eight beakers for the sampling of particles lost during the saturation phase and eroded particles carried away with the effluent. At the overflow outlet of the effluent tank, water falls into a beaker that is continuously weighed to determine injected flow rate.

Testing materials

To obtain a large range of suffusion susceptibility, 18 nonplastic and low-plasticity soils are selected for their different grain-size distributions and different grain shapes. Seven soils come from

Table 1. Properties and potential susceptibility of tested soils.

Soil	φ (°)	Finer KL (%)	V_{BS} (g / 100 g)	min (H/F)	d_5 (mm)	d_{15} (mm)	d_{20} (mm)	d_{50} (mm)	d_{60} (mm)	d_{90} (mm)	C_u	G_r	P (%)	Potential susceptibility (Marot et al. (2016) criterion)
1	44	23	0.1	0.125	0.14	0.294	0.45	2.97	3.27	3.97	14.86	1.6	0.64	U
4	44	16.5	0.07	0.094	0.193	0.445	2.08	3.12	3.347	3.99	11.42	2.67	0.36	U
5	44	25	0.15	0	0.14	0.126	0.45	2.97	3.27	3.97	43.75	8	3.34	U
6	44	25	0.11	0.12	0.193	0.276	2.08	3.12	3.347	3.99	15.88	1.6	0.7	U
B	44	25	0.163	0.035	0.08	0.21	0.15	4.12	4.55	5.86	19.58	2.5	1.6	U
C	43	27.5	0.179	0.034	0.13	0.198	0.389	2.92	3.25	3.97	20.53	2.5	1.7	U
DR-A	45	20	0.13	0.109	0.094	0.148	0.25	1.563	1.692	2.633	14.91	2.4	1.7	S
DR-B	45	25	0.163	0	0.08	0.126	0.151	2.412	2.712	4.727	26.03	4.8	3.3	U
DR-C	45	25	0.163	0	0.08	0.126	0.151	2.99	3.671	5.645	35.25	4.8	3.3	U
G3-11	44	25	0.163	0	0.084	0.127	0.153	2.924	3.25	3.965	30.53	6	2.7	U
G3-13	44	15	0.098	0	0.1	1.5	2.127	3.15	3.362	3.993	25.04	6	1.6	U
G3-14	44	20	0.13	0	0.094	0.145	0.25	3.046	3.309	3.98	29.17	6	1.7	U
3	40	51.84	1.00	0.452	0.014	0.102	0.17	0.542	0.889	3.845	22.23	1	12.12	S
R1	44	15.26	0.11	0.593	0.145	0.315	0.63	2.627	3.029	4.483	13.17	1	0.59	U
R2	43	25.04	0.11	0.195	0.094	0.157	0.263	2.59	3.013	4.484	24.50	1	1.2	U
CH-5	49	60.01	0.41	0.413	0.094	0.224	0.263	0.549	0.75	3.629	4.25	1	3	S
CH-10	49	40.61	0.291	0.443	0.186	0.301	0.368	1.381	3.178	8.354	12.92	1	1	S
CD	37	76.46	0.70	0.11	0.0062	0.026	0.039	0.135	0.182	1.461	10.11	1	29.57	S

Note: Finer KL and min(H/F) are based on Kenney and Lau's (1986) criterion. G_r and P are based on Chang and Zhang's (2013) criterion. φ, internal friction angle; V_{BS}, blue methylene value; F, mass percentage of grains lower than d; H, mass percentage of grains between d and $4d$; C_u, uniformity coefficient; G_r, gap ratio (for widely graded soils, $G_r = 1$); P, percentage of particles smaller than 0.063 mm; U, unstable; S, stable.

Table 2. Properties of specimens.

Soil	Tested specimen	Specimen height (mm)	Dry unit weight (kN/m³)	Applied hydraulic gradient (m/m)	Injected flow (mL/min)	Initial hydraulic conductivity 10^{-5} (m/s)	Final hydraulic conductivity 10^{-5} (m/s)
1	1-T-1	50	16.43	0.4–3	—	3.2	7.0
4	4-T-1	50	16.13	0.1–1.5	—	—	21.3
	4-T-2	100	16.13	0.043–0.705	—	—	140.0
5	5-T-1	50	17	0.4–4	—	—	10.5
	5-T-2	100	17	0.012–0.81	—	—	163.0
6	6-T-1	50	17	0.094–7.50	—	—	0.3
	6-T-3	100	17	0.07–1.13	—	—	21.8
B	B-q1	50	17.39	—	1.60	1.6	0.8
	B-q2	50	17.39	—	12	8.2	6.7
	B-i1	50	17.39	0.1–6	—	2.0	13.3
	B-i2	50	17.39	1–10	—	2.6	7.2
	B-90a	50	17.39	0.38–2.04	—	2.0	13.3
	B-90b	50	17.39	0.77–1.98	—	3.9	53.2
C	C	50	17.39	0.1–7	—	1.4	6.5
DR-A	DR-A	50	17.87	0.1–16	—	2.2	1.4
DR-B	DR-B	50	16	0.1–7	—	4.1	11.6
DR-C	DR-C1	50	16	0.1–7	—	5.8	9.1
	DR-C2	50	16	0.1–7	—	2.8	14.3
G3-11	G3-11	50	16	0.1–5	—	7.3	3.5
G3-13	G3-13	50	16	0.1–6	—	14.5	14.9
G3-14	G3-14	50	16	0.1–8	—	4.6	13.8
3	3-T-1	100	17	0.106–4.65	—	6.0	7.2
	3-T-2	100	15.5	0.106–4.65	—	12.0	10.0
R1	R1-90b	50	17.39	1–11	—	3.4	9.7
R2	R2-90a	50	17.39	0.1–6	—	3.7	13.5
	R2-90b	50	17.39	1–8	—	2.4	15.7
	R2-97b	50	18.74	1–12	—	1.5	6.2
	R2-97d	50	18.74	—	1.25	1.3	1.0
CH-5	CH-5	50	16.54	0.1–14	—	9.0	6.1
CH-10	CH-10	50	18.90	0.1–16	—	8.0	1.6
CD	CD	100	19.14	0.06–6.02	—	3.0	0.1

existing earth structures: soils named DR-A, DR-B, DR-C, and 3 come from different French dikes; two natural soils from a French dike were sieved with two different maximum diameters, which are 5 and 10 mm for soils CH-5 and CH-10, respectively; soil named CD is a till from Canada, which is used for a core of a dam currently under construction. Eleven soils were created by mixing different nonplastic soils: seven soils (1, 6, B, C, G3-11, G3-13, G3-14) are composed of mixtures of sand S1 and gravel G3 (marketed by Sablière Palvadeau, France); soil 4 is created by the mixture of Fontainebleau sand and gravel G3; soil 5 is the mixture of sand S1,

Fig. 3. Time series of hydraulic gradient (tests B-q1, B-i1). [Colour online.]

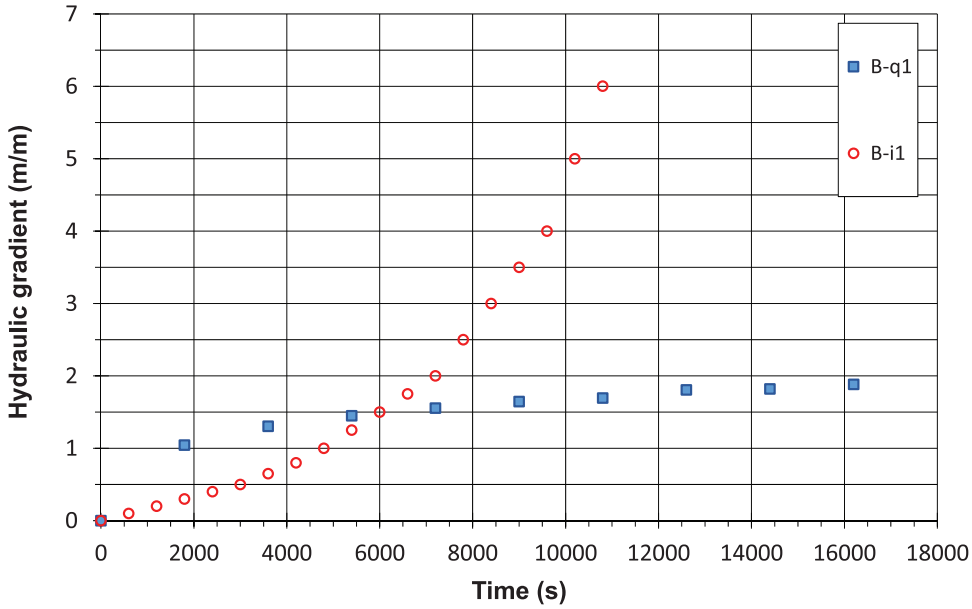

Fig. 4. Time series of hydraulic conductivity (tests B-q1, B-i1). Black spots show time of steady state. [Colour online.]

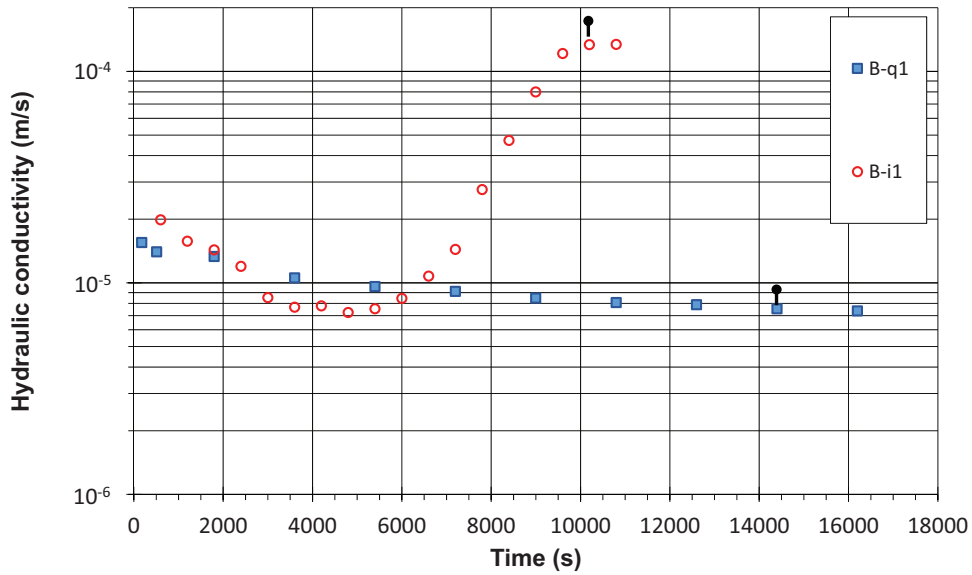

silt Limon Jossigny, and gravel G3; finally, two soils (R1 and R2) are composed of mixtures of sand S1 (d < 0.63 mm) and DR (d > 0.63 mm). A laser diffraction particle-size analyzer was used to measure the grain-size distribution of tested soils with demineralized water and without deflocculating agent (see Figs. 2*a*, 2*b*).

Physical parameters

A set of 14 physical parameters is measured. The selection of these parameters was realized according to the aforementioned identification of predominant parameters. Moreover, the goal of this study is to estimate soil erodibility by physical parameters that may be easily measured on site or on disturbed samples. In accordance with the aforementioned criteria based on grain-size distribution, measured parameters include the uniformity coefficient C_u, the gap ratio G_r, and the percentage P finer than 0.063 mm (see Table 1). The grain-size analysis is also completed by d_5, d_{15}, d_{20}, d_{50}, d_{60}, d_{90} (diameters of the 5%, 15%, 20%, 50%, 60%, 90% mass passing, respectively). For widely graded soils, the fine fraction can be identified within the granular distribution by the minimum value of Kenney and Lau's (1985) ratio min(H/F), and the corresponding fine percentage is named Finer KL. To take into account the influence of grain shape, the internal friction angle φ of mixtures was determined thanks to a direct shear stress device (Marot et al. 2012). The shear tests are carried out on dry aggregates, with density index I_d near to 1. The testing method used is described by standard NF P94-071-1 (Association Française de Normalisation 1994). For low-plasticity soils, the percentage of clay but also the mineralogy and chemical composition of clay give soils a different water sensitivity and a different sensitivity to erosion processes (Haghighi 2012). In consequence, the blue methylene value V_{BS} is also measured because it permits quite easily and rapidly to highlight the water sensitivity of tested soils.

Furthermore, based on the compared criterion of Marot et al. (2016), the potential susceptibility classification is also added in Table 1. Now, according to this criterion, 13 soils appear unstable

Fig. 5. Time series of erosion rate (tests B-q1, B-i1). Black spots show time of steady state. [Colour online.]

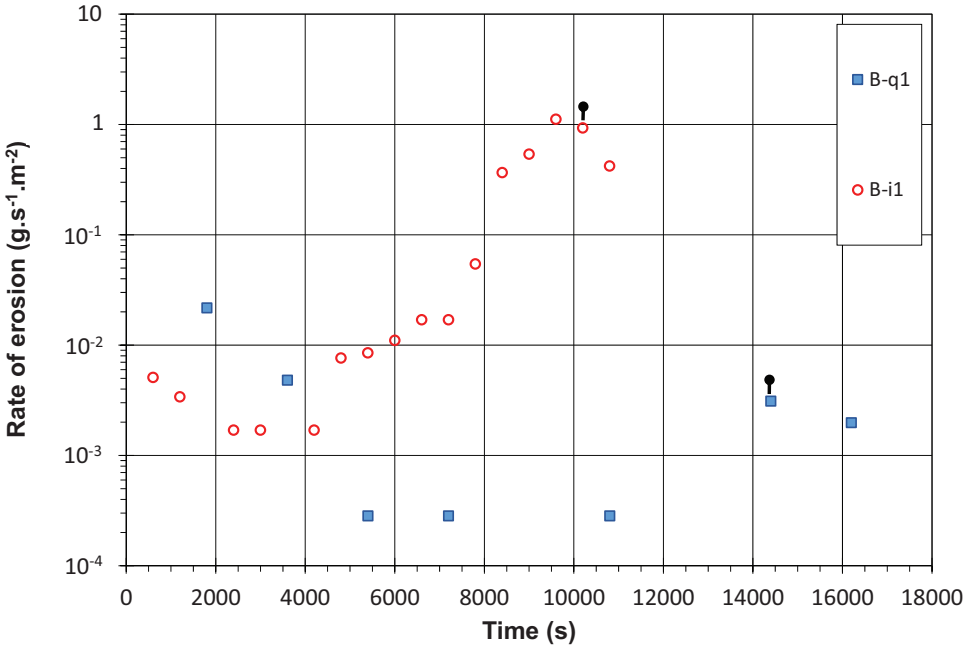

Fig. 6. Cumulative loss of dry mass per unit volume versus cumulative expended energy per unit volume. [Colour online.]

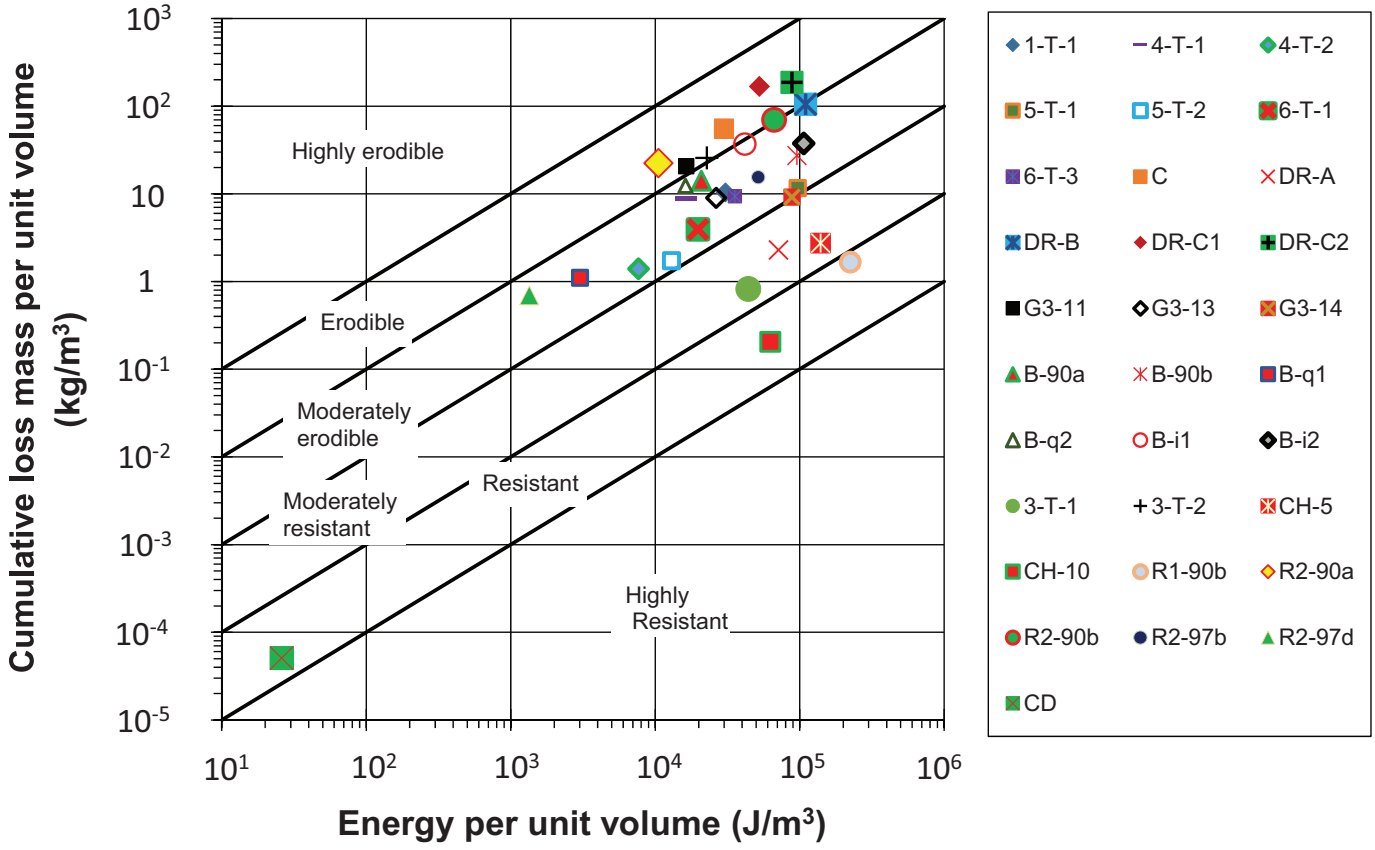

(1, 4, 5, 6, B, C, DR-B, DR-C, G3-11, G3-13, G3-14, R1, R2) and five soils appear stable (DR-A, 3, CH-5, CH-10, CD).

Test procedure and testing program

Thirty-one tests were carried out on samples in oedometric conditions, i.e., with no lateral displacements. As recommended by Kenney and Lau (1985), to reduce preferential flow, a membrane is placed between specimen and metal mold. Six specimens (50 mm in diameter and 100 mm in height; see Table 2) are produced by air pluviation directly into a membrane that is fixed by the metal mold and compacted until obtaining the target specimen volume to reach the target value of dry unit weight. Twenty-five speci-

Table 3. Results of suffusion tests at steady state.

Specimen	Test duration (s)	Loss of mass per unit volume (kg/m³)	Expended energy per unit volume (J/m³)	Erosion resistance index, I_α	Marot et al. (2016) suffusion classification
1-T-1	10800	10.4	30612	3.5	ME
4-T-1	9000	8.9	16249	3.3	ME
4-T-2	10200	1.4	7666	3.7	ME
5-T-1	10800	11.6	96933	3.9	ME
5-T-2	12600	1.7	12971	3.9	ME
6-T-1	15180	4.0	19745	3.7	ME
6-T-3	9420	9.4	35657	3.6	ME
B-q1	14400	1.1	3014	3.4	ME
B-q2	9000	12.4	16228	3.1	ME
B-i1	10200	37.0	41733	3.1	ME
B-i2	5400	37.6	106626	3.5	ME
B-90a	7200	14.1	20907	3.2	ME
B-90b	4200	27.4	95647	3.5	ME
C	11033.4	55.6	30000	2.7	E
DR-A	19877.6	2.3	71346	4.5	MR
DR-B	12020.3	105.0	109684	3.0	ME–E
DR-C1	12582.6	168.5	52579	2.5	E
DR-C2	10820.2	186.6	88308	2.7	E
G3-11	10485.5	20.7	16340	2.9	E
G3-13	8418.8	9.0	26402	3.5	ME
G3-14	12020.7	9.2	88349	4.0	MR–ME
3-T-1	11867.6	0.8	44134	4.7	MR
3-T-2	11160	25.8	22737	3.0	E
R1-90b	6600	1.7	224525	5.1	R
R2-90a	9000	22.3	10536	2.7	E
R2-90b	3600	69.9	66522	3.0	ME–E
R2-97b	5400	15.5	51643	3.5	ME
R2-97d	12600	0.7	1344	3.3	ME
CH-5	16828	2.8	139755	4.7	MR
CH-10	14406.9	0.2	62931	5.5	R
CD	12600	$5(10^{-5})$	26	5.7	R

Note: ME, moderately erodible; E, erodible; MR, moderately resistant; R, resistant.

mens are prepared using a single-layer semi-static compaction technique (Camapum De Carvalho et al. 1987) with a 50 mm diameter and 50 mm high mold. Each specimen is wrapped in a membrane, and then closed inside the metal mold. After this step, carbon dioxide is upwardly injected, followed by the upwardly saturation phase, which requires approximately 24 h. Finally, all specimens are subjected to a seepage flow in a downward direction with deaerated and demineralized water. Two types of hydraulic loading are used: multi-staged hydraulic gradient condition, which consists of increasing the hydraulic gradient by steps, and flow-rate-controlled condition. For soils 3 and R2, two different values of initial dry unit weight are used. Table 2 indicates the initial dry unit weight of specimens and the values of applied hydraulic gradient or injected flow rate for the tested specimens. The repeatability of tests was verified by performing two tests under identical conditions: DR-C1 and DR-C2.

Suffusion test results

Thanks to the measurements of seepage flow and pressure gradient, and based on Darcy's law, it is possible to compute the hydraulic conductivity.

The initial and final values of hydraulic conductivity measured during each test are detailed in Table 2. The repeatability of the seepage test can be validated by comparing the initial and final values of hydraulic conductivity for tests DR-C1 and DR-C2, which are in good agreement. Figure 3 shows the time evolution of hydraulic gradient for soil B according to the different types of hydraulic loading, and Fig. 4 shows the corresponding evolutions of hydraulic conductivity. When the applied hydraulic gradient is increased by steps (test B-i1), the hydraulic conductivity first decreases. The second phase of hydraulic conductivity evolution is characterized by a rapid increase (by a factor of 18 for this test). Finally, the hydraulic conductivity reaches a constant value. Figure 4 shows also the slow decrease with the time of the hydraulic conductivity, which is measured under a constant-flow-rate-controlled test (test B-q1). Thus, some variation in the hydraulic loading appears necessary to produce the second increasing phase of the hydraulic conductivity.

The comparison of time evolution of hydraulic conductivity with time evolution of erosion rate can provide further information to improve the understanding of the suffusion process. The rate of erosion is expressed per unit cross section by

$$\dot{m} = \frac{m_{\text{eroded}}(\Delta t)}{s\Delta t} \quad (3)$$

where $\dot{m}$ is the rate of erosion ($g{\cdot}m^{-2}{\cdot}s^{-1}$), $m_{\text{eroded}}(\Delta t)$ is the mass of eroded particles for the duration Δt (s), and s (m^2) is the cross section of the specimen.

The rate of erosion versus time is plotted in Fig. 5 for tests B-q1 and B-i1. The decrease of hydraulic conductivity is systematically accompanied by a decrease of erosion rate, which suggests that some detached particles can be filtered within the soil itself. This filtration may induce a clogging of several pores and then a decrease of the hydraulic conductivity. In multi-staged hydraulic gradient condition (test B-i1), a rough increase of the erosion rate occurs simultaneously with the increase of the hydraulic conductivity, confirming the assumption of a clogging firstly restricting the water flow and then blown by the seepage flow itself. Thus, the predominant process during this second phase seems to be the detachment and transport of solid particles. Finally, hydraulic

Fig. 7. Representation of variables in (*a*) factor plane F1–F2 and (*b*) factor plane F2–F3. [Colour online.]

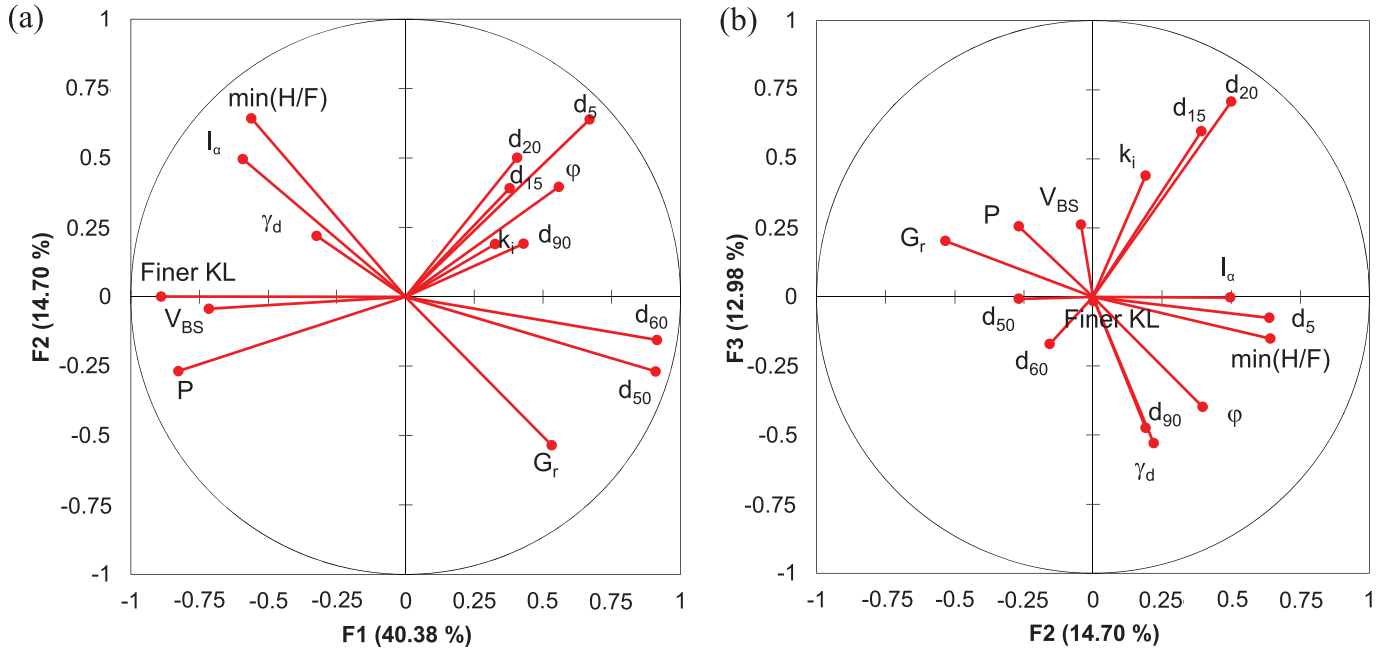

conductivity tends to stabilize while the erosion rate decreases. This third phase could be explained by the presence of preferential flows created by the erosion process leading to a steady state, which is pointed out by black spots in Figs. 4 and 5.

Therefore, these results show that the history of the hydraulic loading has a significant influence on the hydraulic behavior of the specimens and on the development of the suffusion. Moreover, the erosion phenomenon of suffusion appears as a combination of three processes: detachment, transport, and possible filtration of finer fraction.

For characterizing the erosion susceptibility, the cumulative expended energy per unit volume and the cumulative loss of dry mass per unit volume (which includes the mass lost during the saturation phase and the eroded mass) are determined at the end of the test, which is defined by the steady state. The results of all tested specimens are shown in Fig. 6 with the corresponding susceptibility categories. Table 3 details test duration and corresponding values of cumulative loss of dry mass per unit volume, expended energy per unit volume, and erosion resistance index, computed by eq. (2) for all realized tests. The accuracy of the erosion resistance index measurement is evaluated to ±0.02. Moreover, the repeatability tests DR-C1 and DR-C2 lead to an erosion resistance index equal to 2.5 and 2.7, respectively. This discrepancy of 0.2 is due to the measurement accuracy but also to the accuracy related to the specimen creation. Thus, this value is used to define the borders of susceptibility I_α ± 0.1 between two classifications, which are indicated in Table 3. It is worth noting that for a given soil and a given initial dry unit weight (see soils B and R2 in Table 3), the corresponding value of erosion resistance index, and then the corresponding suffusion susceptibility classification, can be determined with accuracy for different hydraulic loadings. Even if the tests were performed with different specimen heights (soils 4–6), the erosion resistance index values are in good agreement. According to the suffusion susceptibility classification, R1-90b, CH-10, and CD are resistant, three specimens (DR-A, 3-T-1, CH-5) are moderately resistant, G3-14 is between moderately resistant and moderately erodible, 16 specimens are moderately erodible (1-T-1, 4-T-1, 4-T-2, 5-T-1, 5-T-2, 6-T-1, 6-T-3, B-q1, B-q2, B-i1, B-i2, B-90a, B-90b, G3-13, R2-97b, R2-97d), two are between moderately erodible and erodible (DR-B and R2-90b), six are erodible (C, DR-C1, DR-C2, G3-11, 3-T-2, R2-90a).

Fig. 8. Erosion resistance index, predicted values (with 14 parameters) versus measured values. [Colour online.]

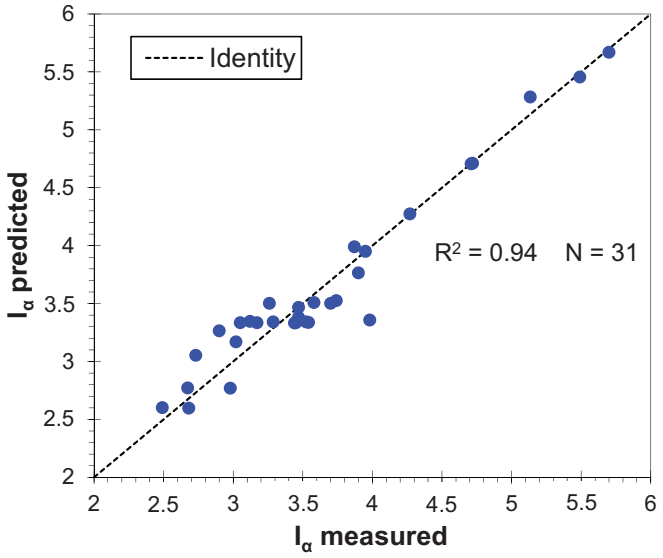

Discussions

Comparison between suffusion susceptibility classification and criteria based on grain size

From the criterion of U.S. Army Corps of Engineers (1953), it is not possible to estimate the potential susceptibility classification because suffusion test results showed that soils 1, 4, and 6 are moderately erodible, whereas their values of C_u are lower than 20. Further, a value higher than 20 can be associated with moderately resistant soil (soil 3). Thanks to the re-evaluation and the identification of less conservative grain-size-based criteria proposed by Marot et al. (2016), the potential susceptibility classification and the suffusion susceptibility classification are in general in agreement for most of tested soils. However, a soil classified as unstable by the potential susceptibility classification (Marot et al. 2016) can be either moderately resistant – moderately erodible (soil G3-14),

Fig. 9. Erosion resistance index, predicted values versus measured values for (*a*) gap-graded soils (with nine parameters) and (*b*) widely graded soils (with seven parameters). [Colour online.]

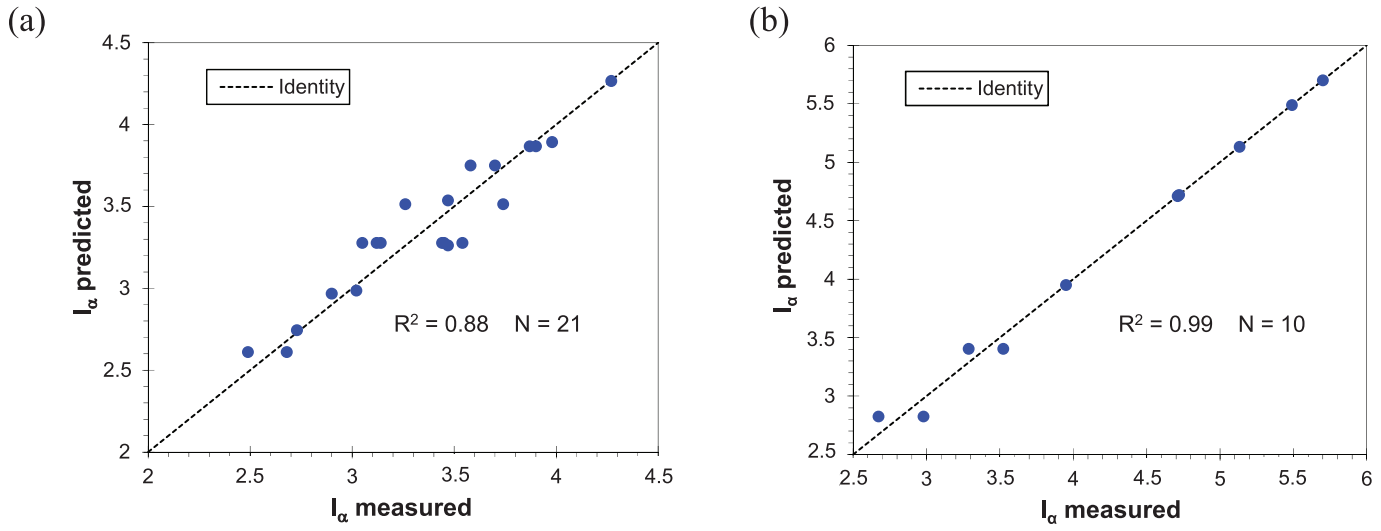

moderately erodible (soil R2), or erodible (soils C, DR-C, G3-11). In the same manner, stable classification corresponds to suffusion susceptibility between moderately resistant (soils DR-A, CH-5) and resistant (soils CH-10, CD). Moreover, the classification of specimen R1-90b based on grain size is unstable, and its suffusion susceptibility is resistant. On the contrary, specimen 3-T-2 is classified as stable, whereas its suffusion classification is erodible. From the same soil but with a higher initial dry unit weight, specimen 3-T-1 is moderately resistant. Thus, these results show the necessity for suffusion susceptibility estimation to take into account physical parameters in addition to grain-size distribution.

Principal component analysis

In conformity with the aforementioned identification of predominant parameters, the physical parameters used in this statistical analysis include the dry unit weight of the soil γ_d, the internal friction angle φ, and the blue methylene value V_{BS}. For the characterization of the grain-size distribution, 10 variables are used: the minimum value of ratio H/F min(H/F), gap ratio G_r, Finer KL, P, d_5, d_{15}, d_{20}, d_{50}, d_{60}, and d_{90}. As the potential susceptibility classification based on the uniformity coefficient C_u is not consistent with suffusion test results, this parameter is not used for the statistical analysis. All aforementioned parameters are related to the soil properties, but the suffusion process is a fluid–solid interaction. Thus, it seems to be interesting to complete the soil description by the initial hydraulic conductivity k_i, although its measurement is more binding than the measurement of the other parameters.

In the principal component analysis, each parameter is represented in a factor space, assuming a linear correlation between the variables. The geometrical representation associates a vector to each parameter, and the scalar product of two associated vectors is equal to the correlation coefficient of the two parameters. An automatic classification is used to define all variables according to the most useful factors. Figures 7*a* and 7*b* show the 14 parameters and the erosion resistance index I_α in two first-factor planes F1–F2 and F2–F3, respectively. From these figures, it can be observed that no parameter is linearly correlated with erosion resistance index. However, the following variables are close to each other on both factor planes: d_{15} and d_{20}, and to a lesser extent d_{50} and d_{60}. This means that they are significantly positively correlated with each other. Gap ratio G_r and min(H/F) appear negatively correlated, as they are on the opposite side of the center.

Multi-variate analysis

By leading a multi-variate analysis, a correlation with erosion resistance index and the 14 aforementioned parameters is proposed:

$$(4)\quad I_\alpha = -13.57 + 0.43\gamma_d + 0.18\varphi - 0.02\ \text{Finer KL} + 0.49V_{BS} + 189.70k_i + 3.82\ \min(H/F) + 0.18P + 0.28G_r + 19.51d_5 + 1.06d_{15} - 0.84d_{20} + 0.81d_{50} - 0.98d_{60} - 0.10d_{90}$$

The obtained correlation coefficient between the prediction and the measurement is $R^2 = 0.94$ for a sample size $N = 31$. Figure 8 shows the erosion resistance index values, computed by eq. (4), versus the measured values.

Ten parameters (γ_d, φ, V_{BS}, G_r, k_i, min(H/F), P, d_5, d_{15}, d_{50}) contribute to eq. (4) with positive sign. On the contrary, the terms with Finer KL, d_{20} d_{60}, and d_{90} are negative. Because of the coupling between several parameters, it is difficult to evaluate the contribution of each one.

From the principal component analysis, a reduction of the number of physical parameters can be performed by eliminating d_{15}, d_{50}, and min(H/F), which are close or opposite on both factor planes to d_{20}, d_{60}, and G_r, respectively (see Figs. 7*a* and 7*b*). Moreover, as the goal of this study is to optimize the experimental campaign by using only quite easily measured parameters, the initial hydraulic conductivity is not used. Finally, thanks to the values of gap ratio, it is possible to distinguish the gap-graded soils (characterized by $G_r > 1$) from the widely graded soils. A new multi-variable analysis can permit building a correlation with the corresponding reduced number of physical parameters. For gap-graded soils, the statistical analysis on 21 specimens leads to the following expression:

$$(5)\quad I_\alpha = -37.62 + 0.67\gamma_d + 0.64\varphi + 0.09\ \text{Finer KL} - 0.03V_{BS} - 1.43P + 0.63G_r + 0.76d_5 - 0.97d_{60} + 0.61d_{90} \qquad (R^2 = 0.88, N = 21)$$

For widely graded soils, the new correlation is

$$(6)\quad I_\alpha = -26.34 + 0.43\gamma_d + 0.66\varphi - 0.16\,\text{Finer KL} + 1.15V_{BS} + 0.37P + 6.82d_5 - 1.26d_{60} \qquad (R^2 = 0.99, N = 10)$$

The erosion resistance index values computed by eqs. (5) and (6) are plotted versus the measured values in Figs. 9*a* and 9*b*, respectively. If we consider the values of parameters and associated factors in eqs. (5) and (6), it is worth noting the key contribution of the dry unit weight and the internal friction angle. This result is consistent with the coupled influence of grain-size distribution, grain shape, and porosity on both aforementioned parameters and also on suffusion susceptibility.

Conclusions

A specific erodimeter is used to study the suffusion susceptibility of 31 specimens of 18 different soils. Tests realized under different hydraulic loading histories highlight the complexity of suffusion, which appears as the result of coupling effects of three processes: detachment, transport, and filtration. The interpretation of such tests is based on the evaluation of the hydraulic loading thanks to the expended energy on one hand, and the cumulative loss of dry mass for the soil response on the other hand. At the steady state, which corresponds to the invariability of the hydraulic conductivity and the decrease of erosion rate, the energy-based method permits the determination of the suffusion susceptibility, and the erosion resistance index is computed.

The following 14 physical parameters were also measured: the dry unit weight of the soil γ_d, the internal friction angle φ, the blue methylene value V_{BS}, the minimum value of ratio H/F, gap ratio G_r, P, Finer KL, initial hydraulic conductivity k_i, and diameters d_5, d_{15}, d_{20}, d_{50}, d_{60}, and d_{90}. A statistical analysis is performed and shows that no parameter is linearly correlated with the erosion resistance index.

Now by focusing on easily measured parameters and by distinguishing the gap-graded soils and widely graded soils, the multivariate statistical analysis leads to an expression of the erosion resistance index for gap-graded soils with respect to nine physical parameters: γ_d, φ, Finer KL, V_{BS}, P, gap ratio G_r, d_5, d_{60}, and d_{90}; and for widely graded soils, a new correlation erosion resistance index with seven parameters: the dry unit weight of the soil γ_d, φ, Finer KL, V_{BS}, P, d_5 and d_{60}. Thus, this method allows an optimization of any experimental campaign of suffusion susceptibility characterization by reducing the number of variables for the description of this susceptibility.

Acknowledgements

The authors thank the company IMSRN France, the Ministry of Education and Training of Vietnam, the University of Danang Vietnam, the Indonesian Directorate General of Higher Education (DIKTI), and the Sultan Agung Islamic University Indonesia for providing financial support for this work.

References

Association Française de Normalisation. 1994. Sols: Reconnaissance et Essais - Essai de cisaillement rectiligne à la boîte - Partie 1: Cisaillement direct. Standard NFP 94-071-1. Association Française de Normalisation (AFNOR), Saint-Denis, France.

Bendahmane, F., Marot, D., and Alexis, A. 2008. Experimental parametric study of suffusion and backward erosion. Journal of Geotechnical and Geoenvironmental Engineering, ASCE, **134**(1): 57–67. doi:10.1061/(ASCE)1090-0241(2008)134:1(57).

Camapum De Carvalho, J., Crispel, J., Mieussens, C., and Nardone, A. 1987. La reconstitution des éprouvettes en laboratoire; théorie et pratique opératoire. Rapport de Recherche LCPC, **145**.

Chang, D.S., and Zhang, L.M. 2013. Critical hydraulic gradients of internal erosion under complex stress states. Journal of Geotechnical and Geoenvironmental Engineering, **139**(9): 1454–1467. doi:10.1061/(ASCE)GT.1943-5606.0000871.

Fell, R., and Fry, J.J. 2013. Erosion in geomechanics applied to dams and levees. *Edited by* S. Bonelli. Wiley-ISTE, pp. 1–99.

Fell, R., and Fry, J.J. (*Editors*). 2007. The state of the art of assessing the likelihood of internal erosion of embankment dams, water retaining structures and their foundations. *In* Internal erosion of dams and their foundations. Taylor & Francis, London, pp. 1–24.

Foster, M., Fell, R., and Spannagle, M. 2000. The statistics of embankment dam failures and accidents. Canadian Geotechnical Journal, **37**(5): 1000–1024. doi:10.1139/t00-030.

Garner, S.J., and Fannin, R.J. 2010. Understanding internal erosion: a decade of research following a sinkhole event. The International Journal on Hydropower and Dams, **17**: 93–98.

Haghighi, I. 2012. Caractérisation des phénomènes d'érosion et de dispersion: développement d'essais et applications pratiques. Ph.D. thesis, Université Paris-Est.

Kenney, T.C., and Lau, D. 1985. Internal stability of granular filters. Canadian Geotechnical Journal, **22**(2): 215–225. doi:10.1139/t85-029.

Kenney, T.C., and Lau, D. 1986. Internal stability of granular filters: Reply. Canadian Geotechnical Journal, **23**(3): 420–423. doi:10.1139/t86-068.

Li, M., and Fannin, R.J. 2008. Comparison of two criteria for internal stability of granular soil. Canadian Geotechnical Journal, **45**(9): 1303–1309. doi:10.1139/T08-046.

Luo, Y.L., Qiao, L., Liu, X.X., Zhan, M.L., and Sheng, J.C. 2013. Hydro-mechanical experiments on suffusion under long-term large hydraulic heads. Nat Hazards, **65**: 1361–1377. doi:10.1007/s11069-012-0415-y.

Marot, D., Bendahmane, F., Rosquoët, F., and Alexis, A. 2009. Internal flow effects on isotropic confined sand-clay mixtures. Soil & Sediment Contamination, an International Journal, **18**(3): 294–306. doi:10.1080/15320380902799524.

Marot, D., Bendahmane, F., and Konrad, J.M. 2011*a*. Multichannel optical sensor to quantify particle stability under seepage flow. Canadian Geotechnical Journal, **48**(12): 1772–1787. doi:10.1139/t11-074.

Marot, D., Regazzoni, P.L., and Wahl, T. 2011*b*. Energy-based method for providing soil surface erodibility rankings. Journal of Geotechnical and Geoenvironmental Engineering (ASCE), **137**: 1290–1787. doi:10.1061/(ASCE)GT.1943-5606.0000538.

Marot, D., Bendahmane, F., and Nguyen, H.H. 2012. Influence of angularity of coarse fraction grains on internal process. La Houille Blance, International Water Journal, **6**(2012): 47–53. doi:10.1051/lhb/2012040.

Marot, D., Rochim, A., Nguyen, H.H., Bendahmane, F., and Sibille, L. 2016. Assessing the susceptibility of gap-graded soils to internal erosion: proposition of a new experimental methodology. Natural Hazards, **83**(1): 365–388. doi:10.1007/s11069-016-2319-8.

Moffat, R., and Fannin, J. 2006. A large permeameter for study of internal stability in cohesionless soils. Geotechnical Testing Journal, **29**(4): 273–279. doi:10.1520/GTJ100021.

Nguyen, H.H., Marot, D., and Bendahmane, F. 2012. Erodibility characterisation for suffusion process in cohesive soil by two types of hydraulic loading. La Houille Blanche, International Water Journal, **6**: 54–60. doi:10.1051/lhb/2012039.

Perzlmaier, S. 2007. Hydraulic criteria for internal erosion in cohesionless soil. *In* Internal erosion of dams and their foundations. *Edited by* R. Fell and J.J. Fry. Taylor & Francis, pp. 179–190.

Reddi, L.N., Lee, I., and Bonala, M.S. 2000. Comparison of internal and surface erosion using flow pump test on a sandkaolinite mixture. Geotechnical Testing Journal, **23**(1): 116–122. doi:10.1520/GTJ11129J.

Sibille, L., Lominé, F., Poullain, P., Sail, Y., and Marot, D. 2015. Internal erosion in granular media: direct numerical simulations and energy interpretation. Hydrological Processes, **29**(9): 2149–2163. doi:10.1002/hyp.10351.

Skempton, A.W., and Brogan, J.M. 1994. Experiments on piping in sandy gravels. Géotechnique, **44**(3): 449–460. doi:10.1680/geot.1994.44.3.449.

U.S. Army Corps of Engineers. 1953. Filter experiments and design criteria. Technical Memorandum, 3-360, Waterways Experiment Station, Vicksburg.

Wan, C.F., and Fell, R. 2008. Assessing the potential of internal instability and suffusion in embankment dams and their foundations. Journal of Geotechnical and Geoenvironmental Engineering, ASCE, **134**(3): 401–407. doi:10.1061/(ASCE)1090-0241(2008)134:3(401).

List of symbols

C_u	uniformity coefficient
d	grain-size diameter
d_5	diameter of 5% mass passing
d_{15}	diameter of 15% mass passing
d_{20}	diameter of 20% mass passing
d_{50}	diameter of 50% mass passing
d_{60}	diameter of 60% mass passing
d_{90}	diameter of 90% mass passing
d_{max}	maximal particle sizes characterizing the gap in the grading curve
d_{min}	minimal particle sizes characterizing the gap in the grading curve
e	void ratio
E_{flow}	expended energy by seepage flow
e_{max}	maximum value of void ratio
e_{min}	minimum value of void ratio
F	mass fraction of particles finer than d

Finer KL percentage of finer based on Kenney and Lau's criteria
G_r gap ratio
H mass fraction of a grain-size distribution ranging from a diameter d to $4d$
I_d density index
I_α erosion resistance index
k_i initial hydraulic conductivity
$\dot{m}$ rate of eroded dry mass per unit cross section
m_{eroded} mass of eroded particles
min(H/F) minimum value of ratio H and F based on Kenney and Lau's criteria
N number of samples
P percentage of particle smaller than 0.063 mm
P_A pressure at section A
P_B pressure at section B
P_{flow} total flow power
Q volumetric flow rate
R^2 correlation coefficient
s cross section of specimen
V_{BS} blue methylene value
z_A vertical coordinate of the upstream section A of the soil volume
z_B vertical coordinate of the downstream section B of the soil volume
γ_d dry unit weight
γ_w specific weight of water
ΔP pressure drop
Δt duration
Δz difference of vertical coordinates
φ internal friction angle